（2）少量のリポソーム投与による脾T細胞の増殖抑制効果について

今まで,循環血液量の5%v/v投与でも再現性をもって脾T細胞の一過性増殖抑制効果の得られることがわかっていた．今回の検討で,循環血液量の1%v/v１回投与では,抑制効果は観察されないが,1%v/vの投与を12時間間隔で2回投与し，12時間後に摘出した脾T細胞の増殖能を検討した結果,再現性を持って，脾T細胞の増殖抑制効果が観察された.今まで得られた,20%v/vの1回投与での実験であり,脾マクロファージは極めて大量のリポソームを捕捉していると推定される.より具体的には，リポソーム溶液の脂質濃度は7~8g/dlである．ラットの循環血液量の20%v/v投与するという操作をヒトに換算すると，1回に投与する脂質の量は80gとなる．これはヒトが１回の食事で摂取する脂質のおおよそ20倍に相当する．しかしながら，循環血液量の1%v/vの投与量は脂質4gに相当し，これはヒトが１回の食事で摂取する脂質量とほぼ同じである．従って，観察されたT細胞抑制効果は，単に脂質の大量負荷だけで説明する事は困難で，リポソームとう形態で投与されることが重要であると推定できる．また,リポソームの素材となっている脂質の種類も重要であると思われる．

血液代替物としてのHbV溶液中の脂質濃度が記述の如く7~8g/dlであり，それを100ml (循環血液量のおおよそ2%v/vに相当)　ヒトに投与するとおおよそ8gの脂質が負荷されることになる．純粋に血液代替物としての使用を考えるとHbVの1回投与量は少なくとも400ml以上となろう．これは体重70kgの成人の循環血液量の10%弱となる．従って，細網内皮系の細胞の機能が一過性に修飾される状態になる可能性がある．しかしながら,あくまでも一過性であり，いままでの諸々の検討結果から，十分に許容できるものであると考えられよう．

E．結論

ラットに空リポソーム溶液を循環血液量の20%(v/v)相当の量を投与した後に，脾臓を取り出し，Con A刺激を加えて培養し,サイトカイン・ケモカインの産生動態の変化を網羅的に観察した．一部のケモカイン・一部のT細胞由来サイトカイン,IL10,TNF-α, IFN-γの産生亢進があるが，細胞増殖に抑制的に作用するとされるTGF-β1の産生動態は,コントロールと差はない．また,LPS刺激によるIL-1β産生動態の検討から,リポソームの投与による自然免疫系の反応性は影響を受けないと思われる.また，リポソームのT細胞増殖抑制効果には，あきらかな容量依存性があり,リポソームの一過性の薬理効果であると考えられる．

F．健康危険情報

該当なし

G．研究業績

1．論文発表

なし

2. 学会発表

1. 東　寛, 藤原満博, 酒井宏水．人工赤血球製剤の血液学的,免疫学的安全性．第62回日本輸血細胞治療学会総会シンポジウム 輸血治療を補完する人工赤血球製剤の効力と安全性 平成26年５月15~17日　奈良

2. 東　寛, 酒井宏水．人工赤血球(ヘモグロビン小胞体)を構成する脂質２重膜のもつ免疫調節効果について．第21回日本血液代替物学会年次大会　シンポジウム：人工赤血球製剤(ヘモグロビン小胞体)の効能と安全性　H26年12月8-9日　東京

H．　知的財産権の出願、登録状況

該当無し。

別添4-4　　平成26年度　厚生労働科学研究費補助金（創薬基盤推進研究事業）

分担研究報告書

人工赤血球(ヘモグロビン小胞体)製剤の実用化を目指す研究

分担課題：ヘモグロビン小胞体の出血性ショックにおける有用性に関する研究

分担研究者　高瀬 凡平　防衛医科大学校　附属病院 集中治療部・准教授
(臨床教育教授)

研究協力者　木下　学　防衛医科大学校・准教授

研究要旨

出血性ショックにより平均全身血圧が40mmHg以下に低下遷延すると、不可逆性心筋障害が発生しいわゆる“出血性ショック心臓”といわれる致死性の病態を呈するとされている。しかし、致死性不整脈の発生機序に関する検討は少ない。また、人工赤血球の効果も明らかでない。そこで、実験的にこれらを検討した。方法：SD rat (n=42)に30%出血性ショック状態を作成し、非蘇生群、洗浄赤血球（RBC）蘇生群、生理食塩水蘇生群、5%アルブミン蘇生群及び人工赤血球蘇生群（LHb [Hgb=6g, n=5] またはHbV [Hgb=10g, n=5])の５群間で心筋を摘出Tyrode液で灌流後 Na^+ channel 感受性色素を用いたOptical mapping system (OMP)で興奮伝播・活動電位持続時間不均一性（Action potential duration dispersion :APDd)、致死性催不整脈性を検討した。蘇生群では、４群とも全例蘇生に成功した。しかし、生理食塩水、5%アルブミン群ではOMPで著明な左心室伝導遅延とburst pacingによる心室細動が全例で誘発されたのに対し、RBC蘇生群では、伝導遅延・心室細動誘発ともに認められなかった。また、人工赤血球蘇生群でも約80%以上の頻度でこれらの異常は認められなかった。生理食塩水、5%アルブミン群では著明にAPDd値が増大したが、RBC群及び人工赤血球蘇生群では正常に保たれていた。以上より、出血性ショック心臓では、左心室伝導遅延とAPDd増大を惹起し、電気的不安定性から致死性不整脈が誘発されると考えられた。RBC治療はこれら指標の保持・予防効果を有した。さらに人工赤血球（LHb・HbV）はRBC治療と同等な治療効果を有する可能性が示唆された。

A．研究目的

これまでの多くの研究や臨床診療において心筋機能障害や心不全は遷延する出血性ショック伴って頻繁に認められるとされている。これらは、出血性ショックからの一時的回復後の予後不良及び出血性ショック時の致死的血行動態破綻に関わる。先行研究によると出血性ショックに伴う心筋虚血や心筋低酸素状態が出血性ショック時の致死性心筋機能障害を惹起すると報告されている。出血性ショックの心臓への致命的障害を回避するためには、出血性ショックの心臓への致命的障害を回避するためには、出血性ショックからの迅速な回復や心筋への重篤な虚血や低酸素血症を未然に防ぐ有効な治療が必要である。

また、出血性ショック・蘇生は、心筋全体の虚血・再還流である。さらに、平均全身血圧が40mmHg以下に低下遷延すると、不可逆性心筋障害が発生しいわゆる“出血性ショック心臓”といわ

れる致死性の病態を呈するとも報告されている。しかし、“出血性ショック心臓”の蘇生後の致死性不整脈出現やその病態に関する検討は少ない。そこで、実験的 に30%出血性ショック状態を作成し、5%アルブミン、生理食塩水、洗浄赤血球で蘇生した４群で心筋を摘出Tyrode液で灌流後Na^+ channel感受性色素を用いたOptical mapping systemで興奮伝播・活動電位持続時間不均一性及び致死性催不整脈誘発性を検討するとともに、人工赤血球（LHb [Hgb=6g] またはHbV [Hgb=10g])のこれらの指標に及ぼす治療効果を検討した。

B．研究方法

Sprague-Dawley rats (male; 8 weeks old; 250-300 g; n = 42)の皮下にketamine hydrochloride (5 mg/kg)を投与し麻酔した。麻酔下に気管内挿管し、人工呼吸下で、abdominal aorta catheter挿入、血圧測定するとともにabdominal aorta catheterから脱血し、以下のプロトコールで致死性出血性ショックモデルを作成した（図１）。すなわち、循環血液量25%を15分で脱血、5分間放置後再出血モデルとして、5%を5分かけて再脱血(Total 30% blood loss：不可逆性Shock)を実施した。その後15分間放置したのち、脱血量と同量 ①5%アルブミン（5%アルブミン群)、②生理食塩水（生理食塩水群)、③洗浄赤血球（洗浄赤血球群)、④人工赤血球（人工赤血球蘇生群: LHb [Hgb=6g, n=5] またはHbV [Hgb=10g, n=5]）で蘇生した。また、⑤非蘇生群も対照群として作成した（① - ③、⑤各群、n=8；④群、n=10)。

(1) Optical mapping analysis 法と不整脈誘発法

Ratsを麻酔後、正中切開にて開胸し、迅速に心臓を摘出した。大動脈から冠動脈洞にカニューレを挿入した。酸素化し37度に保温したTyrode溶液（$CaCl_2$ [2], NaCl [140], KCl [4.5], dextrose [10], $MgCl_2$ [1], and HEPES [10, pH 7.4] , in mmol/L）にて直ちに潅流した。さらに、Tyrode溶液を一定容量で潅流している水槽に心臓を固定し、大動脈に挿入したカニューレからNa感受性蛍色素（di-4-ANEPPS [15 μmol/L]）を約40ml、２分間かけて潅流染色した。さらに、心臓の拍動を停止させるため2.3-butanedione monoxime (Wako Chemical, Tokyo, Japan, 20 mM)を潅流した。Optical mapping analysisはhigh-quality charge couple device (CCD) camera (Leica 10447050, Geneva, Switzerland) を用いて4秒間撮像した。撮像は心筋が洞調律であることを確

図1

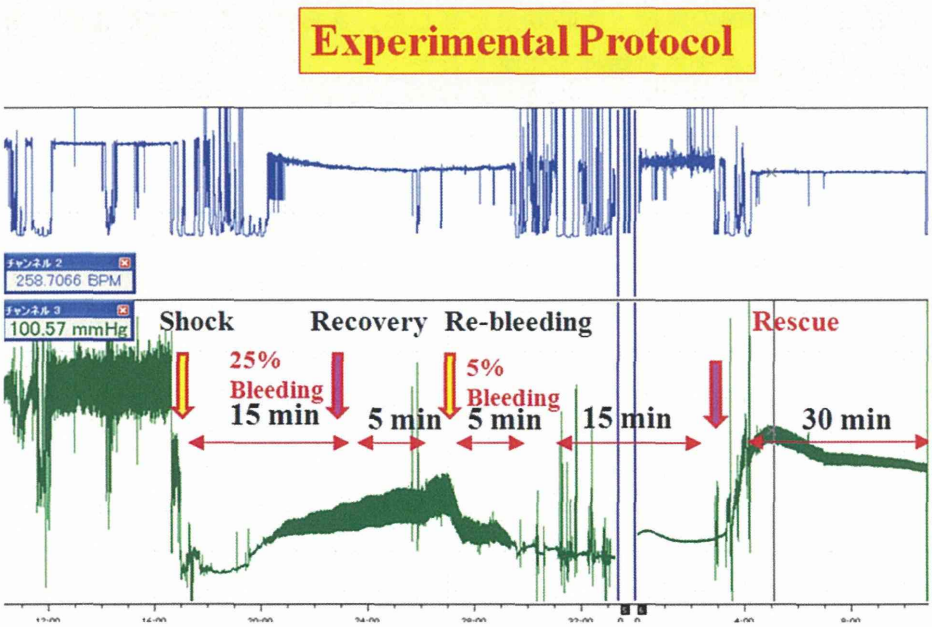

認してから、左心室、右心室外膜面の興奮伝播時間(ms)と伝播様式、得られた活動電位持続時間(APD)をcommercialized software (Ultima-6006; Sei Media, Inc., Tokyo, Japan)にて解析した(図２)殊に、左心室心膜面の約5x5mmの関心部位（ほぼ左心室自由壁の中央）を任意に設定し、この部位におけるAPDの分布のヒストグラムと、APDの実波形を記録した。APDはAPD 60msを使用した。ヒストグラムより、最大APDと最小APDの差からAPD不均一性（APD dispersion [ms]）を決定し、出血性ショ

図2

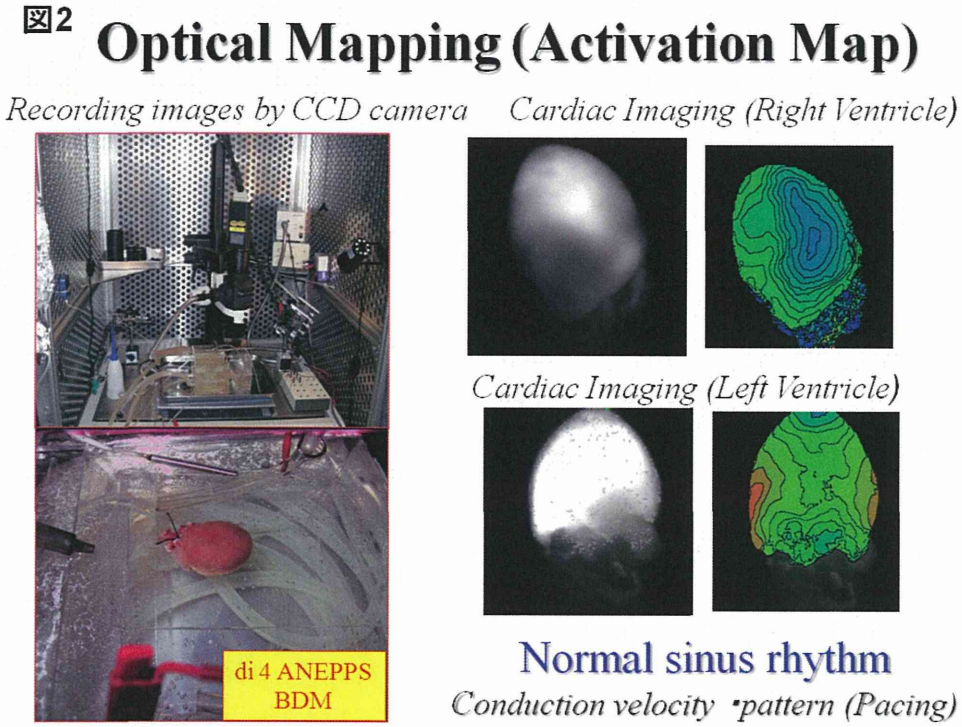

図3

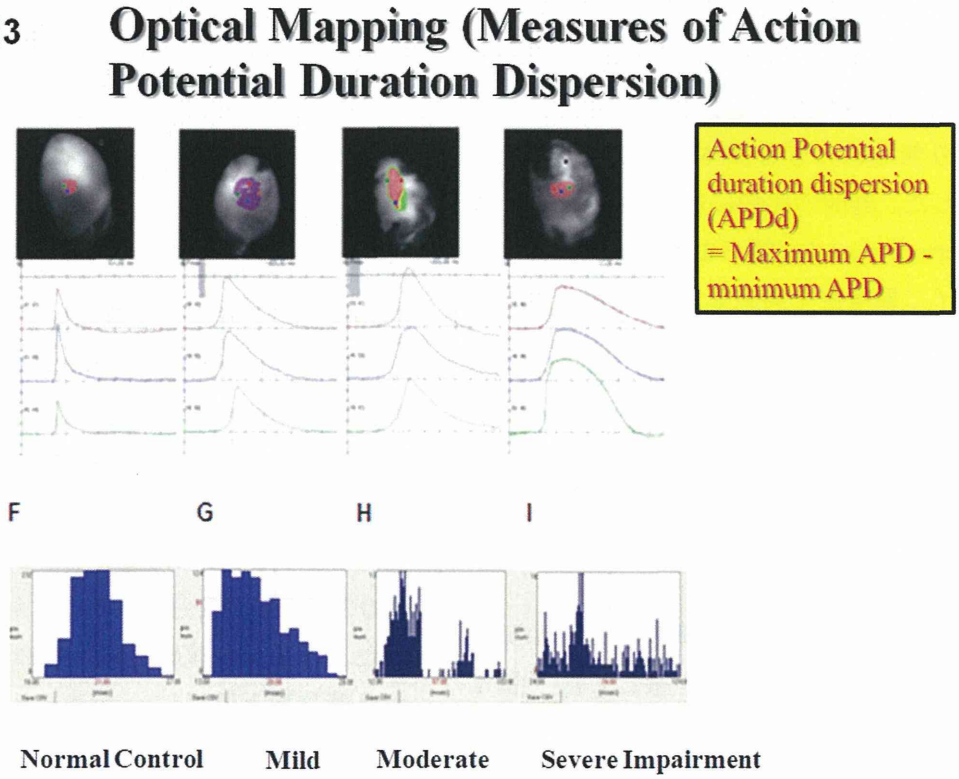

ック蘇生後摘出心臓における、経時的APD dispersion変化を比較した（図３）。

図４

Induction of Lethal Arrhythmias by Burst Stimulation to the Ventricles

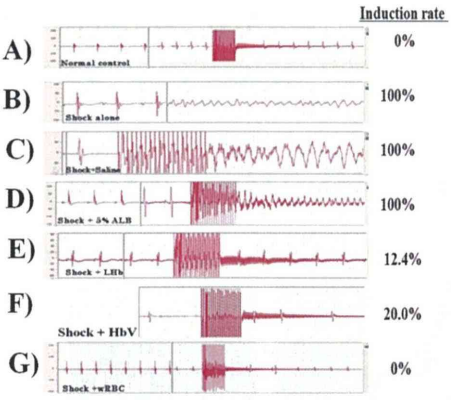

さらに、催不整脈性を調べるために、右心室・左心室の3箇所、すなわち左・右心室心尖部、心臓基部、右室流出路を20回の連続刺激（burst pacing, 5, 50, 100 V; 40-ms interval, 20 trains） 各voltageにて3回づつ施行し、致死性不整脈の誘発の有無を検討した（図４－A）。

(2) 統計学的検討

各群において、興奮伝播時間及びAPD dispersionは平均±標準偏差で表した。興奮伝播様式は異常の有無を、異常有りまたは無しの定性的2分類でその頻度を検討し、致死性不整脈誘発頻度に関しても誘発の有り無しにつき各個体毎に検討し、その頻度を比較した。群間の比較にはANOVA法にて検定し、Bonferroni post hoc補正を実施した。頻度の検定にはカイ二乗検定を実施した。$P<0.05$を推計学的に有意とした。

C．結果

Optical mapping analysis 法による興奮伝播時間・伝播様式及びAPD不均一性と不整脈誘発の結果

非蘇生群では全例Ratsは心室細動または徐脈性不整脈を惹起し、その後心停止を来たした（図４－B）。他の３群では、各蘇生液により全Rats血行動態はショック状態から蘇生された。これら各群のRatsから摘出された心臓の興奮伝播時間・伝播様式をOptical mapping systemにて検討した結果を図５に示した。

図５ Comparison of Activation Map and Action Potential Duration Dispersion after Hemorrhagic Shock

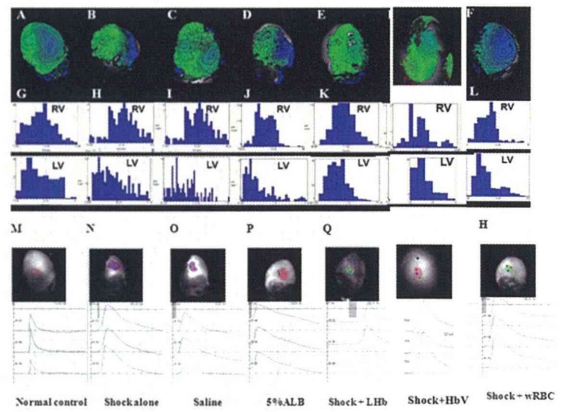

正常Ratsの洞調律における左心室の興奮伝播時間は24±1msであり、伝播様式は図２に示したpatternであった。一方、5%アルブミン群及び生理食塩水群では、ショック状態から蘇生されたにもかかわらず、興奮伝播時間はそれぞれ、35±3ms及び 39±3msとそれぞれ有意かつ著明に延長しており、伝播様式の明らかに正常patternと異なっていた（図５）。しかし、洗浄赤血球群で蘇生したRatsでは、全Rats正常興奮伝播時間（22±3ms）であり、かつ、正常伝播様式であることが認められた。また、人工赤血球蘇生群でも興奮伝播様式は正常興奮伝播様式であり、人工赤血球蘇生群の興奮伝播時間は正常であった（23±5ms）。さらにAPD dispersionは、洗浄赤血球群で全Rats、図３で示したnormal controlと差を認めず（normal control vs. 洗浄赤血球群; 14±2ms vs. 13±3ms, NS）、これに対し、5%アルブミン群及び生理食塩水群では、全Ratsで、図３で示したmoderate または severe impairment patternを示し、APD dispersionはそれぞれ 34±27ms及び38±9msと有意（$P<0.05$）かつ著明に延長していた。人工赤血球蘇生群のAPD dispersionは洗浄赤血球蘇生群と同様にnormal controlと差は認めなか

図６ Comparison of Action Potential Duration Dispersion after Hemorrhagic Shock

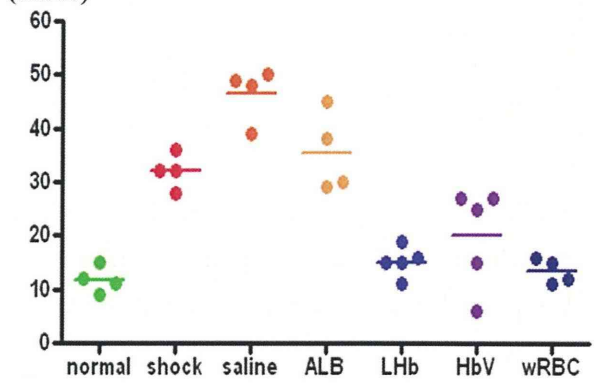

った（14±2ms vs. 18±7ms）。また、活動電位持続時間そのものも正常Rats、洗浄赤血球群及び人工赤血球蘇生群に比較し、5%アルブミン群及び生理食塩水群では著明に延長していることが認められた（図６）。

致死性不整脈の誘発性の検討では、正常Ratsの摘出心臓では通常不整脈が誘発されない両心室へのburst pacing（図４－A）にて、5%アルブミン群及び生理食塩水群蘇生群Ratsでは全Ratsで致死性心室性不整脈（心室細動・心室頻拍）が容易に誘発された（図４－C、D）。しかし、洗浄赤血球群蘇生群及び人工赤血球蘇生群Ratsでは、正常Ratsと同様に致死性不整脈は誘発されなかった（図４－E、F、G）。

D．考案

今回の実験研究は、“出血性ショック心臓”において、洗浄赤血球蘇生及び人工赤血球蘇生が致死性不整脈誘発の抑制効果があり、その機序として心筋興奮伝播時間と伝播様式・活動電位持続時間の均一性を正常に保つ作用が貢献している可能性があることが示唆された。

本研究では、非蘇生群が全Rats死亡する致死性再出血による血性ショックモデル（30%脱血）を用いた、いわゆる“出血性ショック心臓”において、通常臨床現場で用いられる5%アルブミン蘇生群、生理食塩水蘇生群及び洗浄赤血球蘇生群における致死性不整脈の誘発頻度やその機序を摘出心臓に対するOptical mapping systemとburst pacingによる致死性不整脈誘発法で検討した。その結果、5%アルブミン群及び生理食塩水群では血行動態は正常に復し、蘇生に成功したものの、摘出心臓におけるOptical mapping systemでは興奮伝播異常・再分極不均一性を示すAPD dispersion増加が認められ、致死性不整脈の誘発の頻度が増加していた。これらの異常変化は、洗浄赤血球蘇生群では認められなかった。また、人工赤血球蘇生群でも認められなかった。

これまでの報告では、急性血性ショックに伴い、侵襲の大きさに伴った心筋障害が惹起され、血性ショック早期の死亡率に関与しているとされている。これらの心筋障害には、血流の低下及び貧血による心筋虚血そのものの影響に加え、”出血性ショック心臓”に固有の2次的血流障害や代謝異常が関与する可能性を示唆する報告もある。従って、“出血性ショック心臓”では、単に5%アルブミンや生理食塩水による蘇生では、その回復は不十分と考えられる。洗浄赤血球治療群及び人工赤血球蘇生群で、致死性不整脈やその病因となるOptical mapping system解析指標が正常に保たれた。このことは、血性ショック治療において、血行動態の改善のみならず、貧血を改善することにより“出血性ショック心臓”の心筋組織に充分は酸素供給を行うことが重要と考えられる。

本研究を、臨床現場における“出血性ショック心臓”の治療に直結させるには充分とはいえないものの、血性ショック後に遷延する血行動態の不安定性や心不全・致死性不整脈の発生予防に、充分な酸素運搬作用が治療上重要であることを示唆する結果と考えられた。

また、これらは本人工赤血球蘇生が臨床的にも有効である可能性を示唆するものである。

E．結論

出血性ショック心臓では、左心室伝導遅延とAPDd増大を惹起し、電気的不安定性から致死性不整脈が誘発されると示唆された。洗浄赤血球蘇生と人工赤血球蘇生はこれら指標の保持と予防効果を有した。

【補足】

研究課題：凝固障害を伴う家兎の出血性ショックに対する人工赤血球を用いた蘇生救命輸血の効果（木下 学）

【目的】凝固障害を伴う家兎の出血性ショックに対するHbVによる蘇生救命輸血の効果を検討した。

【方法】家兎(2.5 kg)に脱血と赤血球成分のみの返血を繰り返すことで循環血液量のほぼ2倍に相当する400mlの血液交換を行った。血液交換後に、肝臓に穿孔損傷を作成し臓器出血を起こさせた。damage control (出血局所圧迫)と共に、血小板輸血と凝固因子補充を行なった。止血後にHbV(10ml)を輸血し、家兎の濃厚赤血球を輸血する群、5%アルブミンを投与する群とで24時間後の生存率を比較した。

【結果】400mlの脱血返血後、平均血圧40mmHg、Hb5.8g/dl、血小板数40×10^3/μLの貧血と血小板減少を伴う病態となった。これに肝損傷を作製し血小板輸血と凝固因子補充を行った。平均38分で止血が得られたが、25ml(平均)の臓器出血（損傷から10分間）によりHbが4.8 g/dl程度に低下した。その後の蘇生輸血で、濃厚赤血球群とHbV群は70%が救命出来たが、5%アルブミン群は90%が数時間以内に死亡した。

【結論】凝固障害を伴う臓器出血の病態でもHbVは止血凝固に影響せず出血性ショックを改善し、濃厚赤血球と同等の有用性を示した。

F．健康危険情報

該当なし

G．研究業績

(原著論文)

1. Tanaka Y, Takase B. Ventricular electrical remodeling and arrhythmogenic substrate in hemorrhagic shock-induced heart. (Submitted)

2. Watanabe E, Tanabe T, Osaka M, Chishaki A, Takase B, Niwano S, Watanabe I, Sugi K, Katoh T, Takayanagi K, Mawatari K, Horie M, Okumura K, Inoue H, Atarashi H, Yamaguchi I, Nagasawa S, Moroe K, Kodama I, Sugimoto T, Aizawa Y. Sudden cardiac arrest recorded during Holter monitoring: prevalence, antecedent electrical events, and outcomes. Heart Rhythm. 2014:1418-25.

3. Tomiyama H, Yoshida M, Higashi Y, Takase B, Furumoto T, Kario K, Ohya Y, Yamashina A. Autonomic nervous activation triggered during induction of reactive hyperemia exerts a greater influence on the measured reactive hyperemia index by peripheral arterial tonometry than on flow-mediated vasodilatation of the brachial artery in patients with hypertension. Hypertens Res. 2014;37:914-8.

(学会発表)

1. Takase B, Tanaka Y. Cardiac autonomic activity, cardiac function and arrhythmogenic property in hemorrhagic shock heart: Effect of artificial oxygen carrier (American Heart Association Annual Scientific Session 2014, Chicago USA, 2014/11/14-19)

2. Takase B. Possible favorable marker of positive head-up tilt and negative T-wave alternans during test in suspected high risk reflex syncope patients (American Heart Association Annual Scientific Session 2014, Chicago USA, 2014/11/14-19)

3. Takase B. Hamabe A. Effect of calcium-channel blocker on T-wave alternans in coronary artery disease with silent myocardial ischemia and premature ventricular beats
(第29回日本不整脈学会学術大会, Tokyo 2014/7/22-25)

4. Takase B, Tanaka Y, Ishihara M. Myocardial Electrical Remodeling and Arrhythmogenic Substrate in Hemorrhagic Shock-Induced Heart. (The 78th Annual Scientific Meeting of the Japanese Circulation Society, Tokyo, 2014/3/21-23)

5. 高瀬凡平、田中良弘、東村悠子、木下学. 出血性ショックにおける致死性不整脈発生機序とリポソーム封入人工酸素運搬体の効果に関する実験的検討. (第 21 回日本血液代替物学会年次大会. 中央大学理工学部小ホール. 2014 年 12 月 8-9 日).

H. 知的財産権の出願。登録状況（予定を含む）

該当なし

別添 5

表　研究成果の刊行に関する一覧表

刊行書籍又は雑誌名（雑誌のときは雑誌名、巻号数、論文名）	刊行年月日	刊行書店名	執筆者名
Carbon monoxide-bound hemoglobin-vesicles as a potential therapeutic agent for the treatment of bleomycin-induced pulmonary fibrosis. *Biomaterials* 35, 6553-6562 (2014)	2014 年 8 月	Elsevier	S. Nagao, K. Taguchi, H. Sakai, R. Tanaka, H. Horinouchi, H. Watanabe, K. Kobayashi, M. Otagiri, T. Maruyama.
Red blood cells donate electrons to methylene blue mediated chemical reduction of methemoglobin compartmentalized in liposome in blood. *Bioconjugate Chem.* 25, 1301-1310 (2014)	2014 年 7 月	American Chemical Society	H. Sakai, B. Li, W. Lim, Y. Iga.
Normothermic preservation of the rat hind limb with artificial oxygen-carrying hemoglobin vesicles. *Transplantation* 99, 687-692 (2015)	2015 年 4 月	Lippincott Williams & Wilkins	J. Araki, H. Sakai, D. Takeuchi, Y. Kagaya, M. Naito, M. Mihara, M. Narushima, T. Iida, I. Koshima.
Potential electron mediators to extract electron energies of RBC glycolysis for prolonged in vivo functional lifetime of hemoglobin vesicles. *Bioconjugate Chem.* (in press)	印刷中	American Chemical Society	K. Kettisen, L. Bulow, H. Sakai
工赤血球による生体組織への酸素輸送. 「全人力・科学力・透析力に基づく透析医学」」第 6 章: 腎性貧血. pp.369-373 平方秀樹 監修	2014 年	医薬ジャーナル社	酒井宏水
人工赤血球(ヘモグロビン小胞体)微粒子分散液の特徴. *粉体工学* 6, 909-914 (2014)	2014 年 6 月	日本粉体工業技術協会	酒井宏水
人工赤血球で血液不足を解決する日がやってくる. *Self Brand 2015,* 85 (2014)	2014 年	フロムページ	酒井宏水
ヘモグロビンの再利用で赤血球の寿命を延ばす. *Someone* 24, 9 (2014)	2014 年 9 月	リバネス出版	酒井宏水
人工赤血球(ヘモグロビンベシクル)の実現に向けて. *医学のあゆみ* (印刷中)	印刷中	医歯薬出版株式会社	酒井宏水、久禮智子

特許出願

PCT/JP2012/59233 (2012年4月4日出願):　小胞体の製造法.

(2013年度に国内段階移行完了: 米国, インド, 中国, EP, 日本)

報道

日本テレビ「世界一受けたい授業」にて、人工赤血球が紹介された(2014年7月5日, 19:00 – 20:58)

その他

1)　第62回日本輸血・細胞治療学会総会 シンポジウム12「輸血治療を補完する人工赤血球製剤の効力と安全性」2014年5月17日（奈良県新公会堂）

2)　第52回日本人工臓器学会大会 ワークショップ２「人工赤血球製剤の効力と安全性」2014年10月18日（京王プラザホテル札幌）

3)　第21回日本血液代替物学会年次大会 シンポジウム１「人工赤血球(ヘモグロビン小胞体)製剤の効能と安全性」2014年12月8日（中央大学理工学部）

研究成果の刊行物・別冊

(2014. 4. － 2015. 3.)

Biomaterials 35 (2014) 6553–6562

Contents lists available at ScienceDirect

Biomaterials

journal homepage: www.elsevier.com/locate/biomaterials

Carbon monoxide-bound hemoglobin-vesicles for the treatment of bleomycin-induced pulmonary fibrosis

Saori Nagao [a,1], Kazuaki Taguchi [b,1], Hiromi Sakai [c], Ryota Tanaka [a], Hirohisa Horinouchi [d], Hiroshi Watanabe [a,e], Koichi Kobayashi [d], Masaki Otagiri [a,b,f,**], Toru Maruyama [a,e,*]

[a] Department of Biopharmaceutics, Graduate School of Pharmaceutical Sciences, Kumamoto University, Kumamoto 862-0973, Japan
[b] Faculty of Pharmaceutical Sciences, Sojo University, Kumamoto 860-0082, Japan
[c] Department of Chemistry, Nara Medical University, Kashihara 634-8521, Japan
[d] Department of Surgery, School of Medicine, Keio University, Tokyo 160-8582, Japan
[e] Center for Clinical Pharmaceutical Sciences, School of Pharmacy, Kumamoto University, Kumamoto 862-0973, Japan
[f] DDS Research Institute, Sojo University, Kumamoto 860-0082, Japan

ARTICLE INFO

Article history:
Received 26 February 2014
Accepted 13 April 2014
Available online 6 May 2014

Keywords:
Antioxidant
Fibrosis
Inflammation
Liposome
Lung

ABSTRACT

Carbon monoxide (CO) has potent anti-inflammatory and anti-oxidant effects. We report herein on the preparation of a nanotechnology-based CO donor, CO-bound hemoglobin-vesicles (CO-HbV). We hypothesized that CO-HbV could have a therapeutic effect on idiopathic pulmonary fibrosis (IPF), an incurable lung fibrosis, that is thought to involve inflammation and the production of reactive oxygen species (ROS). Pulmonary fibril formation and respiratory function were quantitatively evaluated by measuring hydroxyproline levels and forced vital capacity, respectively, using a bleomycin-induced pulmonary fibrosis mice model. CO-HbV suppressed the progression of pulmonary fibril formation and improved respiratory function compared to saline and HbV. The suppressive effect of CO-HbV on pulmonary fibrosis can be attributed to a decrease in ROS generation by inflammatory cells, NADPH oxidase 4 and the production of inflammatory cells, cytokines and transforming growth factor-β in the lung. This is the first demonstration of the inhibitory effect of CO-HbV on the progression of pulmonary fibrosis *via* the anti-oxidative and anti-inflammatory effects of CO in the bleomycin-induced pulmonary fibrosis mice model. CO-HbV has the potential for use in the treatment of, not only IPF, but also a variety of other ROS and inflammation-related disorders.

1. Introduction

Idiopathic pulmonary fibrosis (IPF) is a chronic and progressive type of fibrous interstitial pneumonia with an unknown cure, except for lung transplantation. Patients with IPF have an estimated median survival of 2–5 years [1–3]. Pirfenidone (5-methyl-1-phenyl-2-[1H]-pyridone) is currently the only orally administered drug approved for clinical use in the treatment of IPF in both the EU and Japan. Recently, the CAPACITY (Clinical Studies Assessing Pirfenidone in idiopathic pulmonary fibrosis: Research of Efficacy and Safety Outcomes) program showed that pirfenidone has a favorable benefit–risk profile, and, as a result, represents an appropriate treatment option for patients with IPF [4]. On the other hand, this multinational, double-blind, placebo-controlled study (CAPACITY006) also showed that pirfenidone treatment does not completely improve the clinically meaningful effects on forced vital capacity (FVC) and survival benefit [4]. In addition, it is well-known there are some significant side effects associated with the use of

Abbreviation: CO, carbon monoxide; HbV, hemoglobin-vesicles; CO-HbV, CO-bound hemoglobin-vesicles; IPF, idiopathic pulmonary fibrosis; FVC, forced vital capacity; ROS, reactive oxygen species; TGF-β, transforming growth factor-β; CO-RM, CO-releasing molecules; HbCO, carboxyhemoglobin; RBC, red blood cell; PEG, polyethylene glycol; BLM, bleomycin; 8-OH-dG, 8-hydroxy-2′-deoxygenase; NO_2-Tyr, nitrotyrosine; TNF-α, tumor necrosis factor-α; IL-6, interleukin-6; IL-1β, interleukin-1β; Nox4, nicotinamide adenine dinucleotide phosphate oxidase 4; Poldip2, polymerase delta interacting protein 2; EMT, epithelial–mesenchymal transition.

* Corresponding author. Department of Biopharmaceutics, Graduate School of Pharmaceutical Sciences, Kumamoto University, Kumamoto 862-0973, Japan. Tel.: +81 96 371 4150; fax: +81 96 362 7690.
** Corresponding author. Faculty of Pharmaceutical Sciences, Sojo University, Kumamoto 860-0082, Japan. Tel.: +81 96 326 3887; fax: +81 96 326 5048.
E-mail addresses: otagirim@ph.sojo-u.ac.jp (M. Otagiri), tomaru@gpo.kumamoto-u.ac.jp (T. Maruyama).
[1] These authors contributed equally to this work.

http://dx.doi.org/10.1016/j.biomaterials.2014.04.049
0142-9612/

pirfenidone, which include photosensitivity (more than 50% of patients) [5]. Therefore, the development of drugs designed to suppress the progression of this disease or to improve respiratory function is of great importance.

Since new pathogenic pathways and mediators of IPF are discovered, the progression of IPF appears to result from a complex combination a number of factors, including inflammation, reactive oxygen species (ROS) and transforming growth factor (TGF)-β. Although recent studies have suggested that the repeated administration of drugs with either anti-oxidative or anti-inflammatory properties would be expected to be useful in the treatment of IPF [6,7], the clinical use of these agents for IPF have not been approved worldwide. This is likely because these agents targeted only one of the many pathogenesis pathways, and, because mechanism responsible for the development of IPF is complex, little alleviation occurs. Therefore, a shift in the effective treatment strategy for IPF from agents that block a single functional action to an agent that can address multiple functions is clearly needed.

Carbon monoxide (CO) possesses anti-inflammatory, anti-oxidant and anti-proliferative effects, and has attracted interest as a possible clinically viable medicinal agent [8,9]. Similar to medical gasses that are routinely used in clinical situations, such as nitric oxide and oxygen, clinical applications of CO take the form of inhaled gaseous therapy and the use of CO-releasing molecules (CO-RM) [10,11]. In fact, several studies have demonstrated the efficacy of inhaled CO and CO-RM in preclinical animal models such as disorders related to inflammation and redox [12–14]. In addition, it was reported that inhaled CO and CO-RM also exerts protective effects in the case of several types of lung diseases, including pulmonary hypertension, asthma and ischemia reperfusion [15–17]. Taking these findings into consideration, CO holds enormous potential for use in the treatment of pulmonary disorders, including IPF. However, CO-RM rapidly liberates CO, with a half-life of 1–21 min, which is extremely short in terms of producing a significant therapeutic impact [18]. To achieve a sustainable therapeutic effect of CO, the continuous or repeated administration of CO-RM would be required. In addition, although high serum carboxyhemoglobin (HbCO) levels can cause several toxicity [19], it is difficult to control the serum HbCO levels as the result of inhaled CO and avoid CO intoxication. Therefore, it should be noted that an alternative pathway for the therapeutic delivery of CO to the lungs is essential in the successful clinical application of CO.

Recent developments in nanotechnology-based carriers, namely, Hemoglobin-vesicles (HbV), would offer great potential for effective CO delivery, and could lead to strategies in the development of new CO donors. To date, several preclinical trials have evaluated the histology, biochemical analysis and pharmacokinetic properties after the single or repeated administration of a putative dose of HbV in rodent, pig and monkey [20–24]. The results show that HbV possesses good biological compatibility (low complement activation) and is promptly metabolized (no accumulation in the body) even after a massive single or repeated infusion. Furthermore, the size of HbV is controlled at ca. 250 nm, because it can prevent capillary plugging, renal excretion and vascular wall permeability. Fortunately, CO easily and stably binds to hemoglobin (Hb) in the form of HbV as well as red blood cell (RBC), because the cellular structure of HbV most closely mimics the characteristics of a natural RBC, in which a highly concentrated Hb is encapsulated within a liposome with polyethylene glycol (PEG). In addition, in a previous study, we reported that CO was exhaled within 6 h after administering CO-bound HbV (CO-HbV) to hemorrhagic-shocked rats [25]. These findings led us to the hypothesis that HbV has the potential for use a carrier of CO to the lungs. Given the known therapeutic effects of CO-HbV on IPF, we decided to first evaluate whether CO-HbV could protect against IPF using an IPF animal model of bleomycin (BLM)-induced pulmonary fibrosis. In subsequent experiments, we investigated the reason why CO-HbV functions to suppress the progression of IPF.

2. Materials and methods

2.1. Preparation of HbV and CO-HbV solution

HbVs and CO-HbV were prepared under sterile conditions, as previously reported [26]. In short, the Hb solution was purified from outdated donated RBC, which was provided by the Japanese Red Cross Society (Tokyo, Japan), and the oxyhemoglobin converted into HbCO by bubbling with CO gas. The lipid bilayer was a mixture of 1,2-dipalmitoyl-*sn*-glycero-3-phosphatidylcholine, cholesterol, and 1,5-bis-*O*-hexadecyl-*N*-succinyl-L-glutamate (Nippon Fine Chemical Co. Ltd., Osaka, Japan) at a molar ratio of 5/5/1, and 1,2-distearoyl-*sn*-glycero-3-phosphatidylethanolamine-*N*-PEG (NOF Corp., Tokyo, Japan) (0.3 mol%). The CO-HbV particles were prepared by the extrusion method, and suspended in a physiological salt solution, filter-sterilized (Dismic, Toyo-Roshi, Tokyo, Japan; pore size, 450 nm). By illumination with visible light under an oxygen atmosphere, CO-HbV was converted to HbV. The HbV particles suspended in physiological salt solution bubbled with nitrogen for storage. The average diameters of the HbV and CO-HbV were maintained at approximately 250 nm *via* stepwise extrusion through cellulose acetate membrane filters with a final pore size of 0.2 μm (Fig. 1). The HbV and CO-HbV suspended in physiological salt solution were at [Hb] = 10 g/dL and [lipid] = 9.0 g/dL. The HbCO rate in CO-HbV was nearly 100%, while that in HbV was less than 5%.

2.2. Production of BLM-induced pulmonary fibrosis mice model

All animal experiments were conducted in accordance with the guidelines of Kumamoto University for the care and use of laboratory animals. To create BLM-induced pulmonary fibrosis model mice, Sea-ICR mice (6 weeks, male; Kyudo Co.,Ltd, Saga, Japan) were intratracheally treated with BLM (5 mg/kg; Nippon Kayaku, Tokyo, Japan) in PBS (1 ml/kg) under anesthesia with chloral hydrate (500 mg/kg) as previous report [27]. Saline, HbV, or CO-HbV was administered *via* the tail vein at 30 min before BLM treatment and 24 h after BLM treatment.

2.3. Plasma biochemical parameters

At 7 and 14 days after the HbV injection, BLM-induced pulmonary fibrosis model mice were anesthetized with ether and collected blood. Blood samples were immediately centrifuged (3000 g, 10 min) to produce plasma. The plasma samples were then ultracentrifuged to remove HbV (50,000 g, 30 min), because HbV interferes with some of the laboratory tests [28]. All plasma samples were stored at −80 °C until used. All plasma samples were analyzed by Clinical Chemistry Analyzer (JEOL, JCA-BM6050, Tokyo, Japan).

2.4. Histological and immunohistochemical analyses

The whole lungs were removed and fixed with 10% phosphate buffered formalin. The tissue was then dehydrated at room temperature through a graded ethanol series and embedded in paraffin. The prepared tissues were cut into 4-μm-thick sections for histological and immunohistochemical evaluation. Hematoxylin and Eosin (HE) stain and Masson's trichrome stain were performed as previously described [27]. The immunostaining for 8-hydroxy-2′-deoxygenase (8-OH-dG) and nitrotyrosine (NO_2-Tyr) were performed as described in a previous report with minor modifications [29]. In short, the primary antibody reaction was conducted below 4 °C overnight, and the secondary antibody reaction at room temperature for 90 min. In addition, the primary antibody containing NO_2-Tyr (Millipore, Tokyo, Japan, cat#: AB5411) and 8-OH-dG [15A3] (Santa Cruz, California, USA, cat#: sc-66036) was diluted 50 fold prior to use. The secondary antibodies for 8-OH-dG and NO_2-Tyr were Alexa Fluor 488 goat anti-rabbit IgG (H + L) (Invitrogen, Eugene, USA, cat#: AB11008) and Alexa Fluor 546 goat anti-rabbit IgG (H + L) (Invitrogen, Eugene, USA, cat#: AB11010), respectively. In each case the secondary antibody was diluted 200 times before use. After the reaction, the slide was observed using Microscope (Keyence, BZ-8000, Osaka, Japan).

2.5. Determination of hydroxyproline level in lung tissues

On day 14 after BLM administration, the left lung was removed and hydroxyproline content was determined as described previously [30]. The absorbance was measured at 550 nm to determine the amount of hydroxyproline.

2.6. Measurement of lung mechanics and FVC

Measurement of lung mechanics and FVC were performed with a computer-controlled small-animal ventilator (FlexiVent; SCIREQ), as described previously [31]. Mice were mechanically ventilated at a rate of 150 breaths/min, using a tidal volume of 8.7 ml/kg and a positive end-expiratory pressure of 2–3 cm H_2O. Total respiratory system elastance and tissue elastance were measured by the snap shot and forced oscillation techniques, respectively.

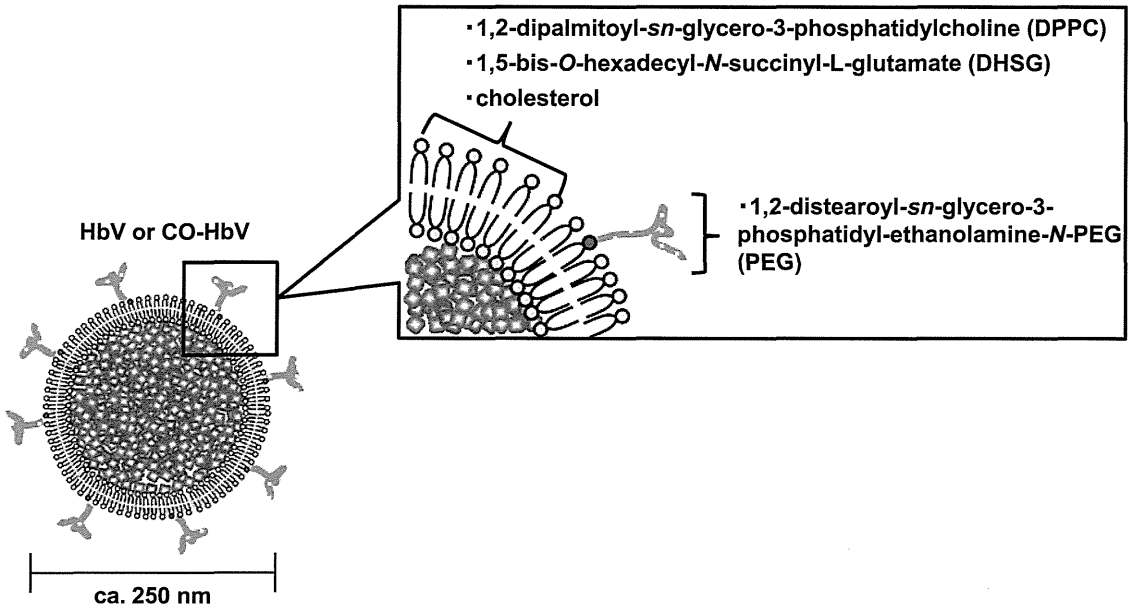

Fig. 1. Structures of hemoglobin-vesicles and its lipid components.

2.7. Counting of cells in bronchoalveolar lavage fluid (BALF)

At days 3 after the BLM administration, BALF was collected as described previously [27]. Total cell number was counted using a hemocytometer. Cells were stained with Diff-Quick reagents (Kokusai Shiyaku, Kobe, Japan), and the ratios of alveolar macrophages, neutrophils, and lymphocytes to total cells were determined. More than 200 cells were counted for each sample.

2.8. Quantification of tumor necrosis factor (TNF)-α, interleukin-6 (IL-6), interleukin-1β (IL-1β) and activated TGF-β1 in lung tissue

At days 7 and 14 after the BLM administration, whole lungs were removed and homogenized in 0.5 ml of buffer (PBS, 1% protease inhibitor cocktail, 10 mM EDTA, 0.05% Tween-20). After centrifugation at 21,000 g for 10 min at 4 °C (twice), the supernatants were recovered. The amount of TNF-α, IL-6, IL-1β on Day 7 and activated TGF-β1 on Day 14 in the supernatant was measured by ELISA kit (TGF-β1 ELISA kit; R&D Systems Inc., Minneapolis, USA, IL-6, TNF-α and IL-1β ELISA kit; Biolegend, San Diego, USA).

2.9. Western blotting analysis

At day 7 after the BLM administration, whole lungs were removed and homogenized in a homogenization buffer composed of 70 mmol/l sucrose, 10 mmol/l HEPES (4-(2-hydroxyethyl)-1-piperazineethanesulfonic acid), 210 mmol/l mannitol, 1 mmol/l EDTA, 1 mmol/l EGTA (ethylene glycol tetraacetic acid), pH 7.5, 200 mmol/l dithiothreitol, and 1% protease inhibitor cocktail. The homogenate was centrifuged at 720 g for 5 min at 4 °C, and the supernatants were recovered. The supernatants were centrifuged at 10,000 g for 5 min at 4 °C and further centrifuged at 100,000 g for 1 h. The resultant pellet is referred to as the crude membrane fraction. After measurement of the protein content, each sample was mixed in a loading buffer (2% sodium dodecyl sulfate, 62.5 mmol/l Tris–HCl and 1% 2-mercaptoethanol). These samples (40 mg) were run on 12.5% sodium dodecyl sulfate polyacrylamide gels, followed by electrophoretic transfer to nitrocellulose membranes. The membranes were blocked by treatment with 5% skimmed milk in PBS for 1 h at room temperature and then incubated with rabbit polyclonal anti-human nicotinamide adenine dinucleotide phosphate oxidase 4 (Nox4) [H-300] (Santa Cruz, California, USA, cat#: sc-30141, 1:500) antibodies, goat polyclonal anti-human $p22^{phox}$ [C-17] (Santa Cruz, California, USA, cat#: sc-11712, 1:600) antibodies, rabbit polyclonal anti-human polymerase delta interacting protein 2 (Poldip2) (Abgent, California, USA, cat#: AP7626b, 1:200) antibodies, or mouse monoclonal anti-human β-actin antibody (1:5000) overnight at 4 °C. The membranes were washed with 0.05% Tween-20 (T-PBS), and a horseradish peroxidase–conjugated anti-goat IgG antibody (Santa Cruz, California, USA, cat#: sc-2768, 1:5000), an anti-rabbit IgG antibody (Santa Cruz, California, USA, cat#: sc-2004, 1:5000), and an anti-mouse IgG antibody (Santa Cruz, California, USA, cat#: sc-2005, 1:10,000) were then used for the detection of the target proteins. SuperSignal Western blotting detection reagents (Thermo Scientific, Rockford, IL) were used for immunodetection.

2.10. Detection of superoxide

Dihydroethidium was used to evaluate lung superoxide concentrations *in situ*, as described in detail elsewhere [32]. After the reaction, the slide was observed under a microscope (Keyence, BZ-8000, Osaka, Japan).

2.11. Statistics

Statistical analyses were performed using the analysis of variance. A probability value of $p < 0.05$ was considered significant.

3. Results

3.1. Evaluation of the optimal dosing of CO-HbV in BLM-induced pulmonary fibrosis

Fig. 2A shows a schematic summary of the experimental protocols used in the study. Pulmonary fibrosis was induced in the mice by a single intratracheal administration of BLM (at day 0) and confirmed 14 days later. In order to determine the optimal dosing of CO-HbV in BLM-induced pulmonary fibrosis, histopathological analysis (HE stain and Masson's trichrome stain) and hydroxyproline levels were evaluated after the administration of CO-HbV at 30 min prior to the BLM treatment and day 1 after the BLM treatment at doses of 250, 500, 1000 and 1400 mg Hb/kg. As shown in Fig. 2B and C, pulmonary fibrosis was suppressed as the result of the administration of CO-HbV and suppression was dose-dependent. The maximum ameliorative effect was achieved at a concentration of 1000 mg Hb/kg.

We also evaluated the toxic effects of CO-HbV administration in BLM-induced pulmonary fibrosis mice. No evidence of the development of signs of hypoxia or abnormal behavior was found when CO-HbV as administered at a dose of 1000 mg Hb/kg. Furthermore, no changes in of serum laboratory parameters reflecting hepatic, renal and pancreatic function were found at 7 and 14 days after CO-HbV administration, except for an elevation in cholesterol levels, compared to the saline treatment in BLM-induced pulmonary fibrosis mice (Table 1). Based on these results, we concluded that the optimal dose of CO-HbV was 1000 mg Hb/kg.

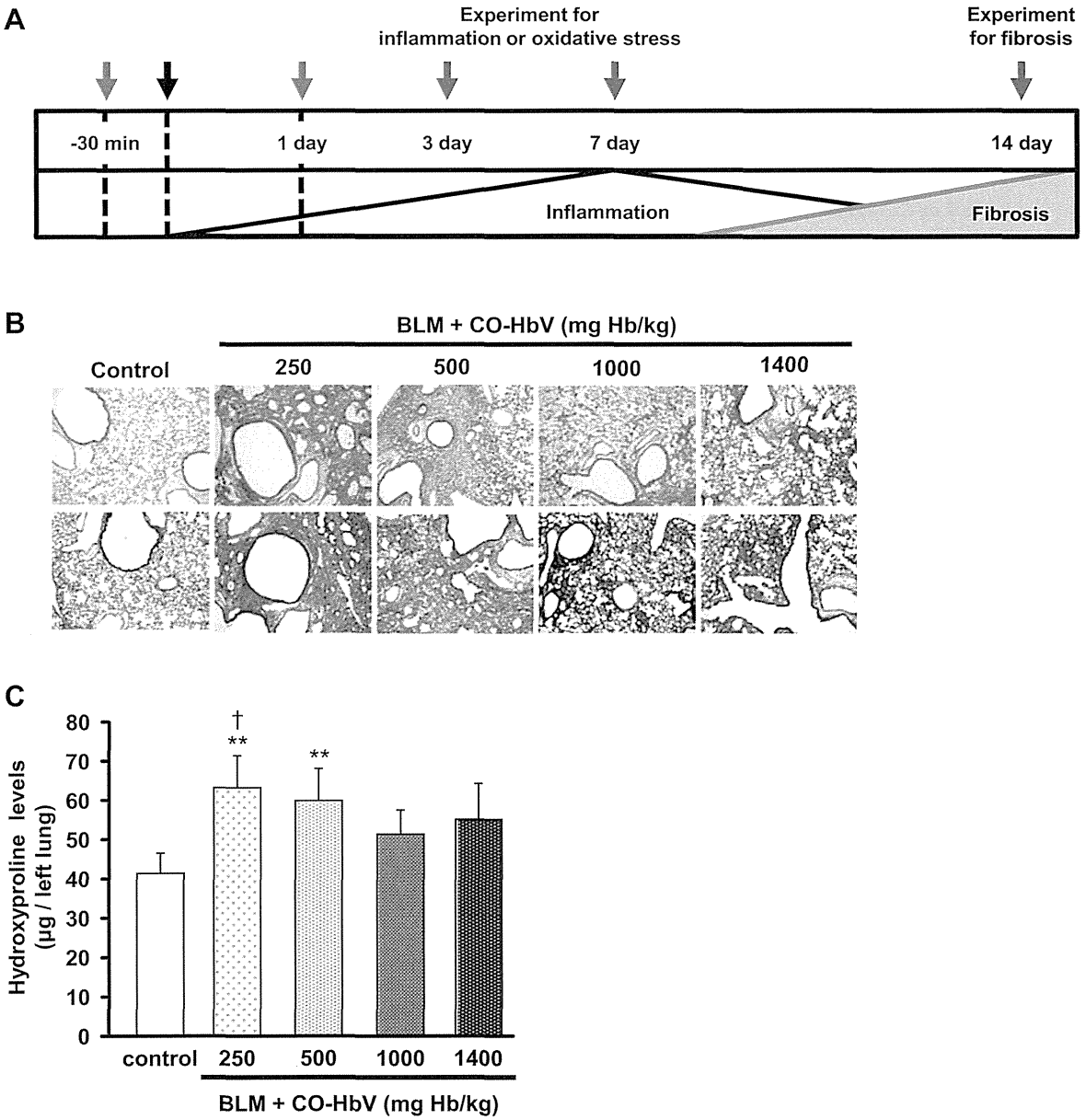

Fig. 2. CO-HbV affects BLM-induced pulmonary fibrosis in a dose-dependent manner. (A) Outline of the experimental design. Mice were treated with bleomycin (BLM, 5 mg/kg) once on day 0. They were also administered by CO-HbV *via* the tail vein at 30 min before BLM treatment and 24 h after BLM treatment. (B) Histopathologic evaluation at after CO-HbV treatment on day 14 in BLM-induced pulmonary fibrosis mice. Sections of pulmonary tissues were prepared on day 14 and subjected to hematoxylin and eosin staining (upper panels) and Masson trichrome staining (lower panels). (C) Hydroxyproline levels in left lung at after CO-HbV treatment on day 14 in BLM-induced pulmonary fibrosis mice. The pulmonary hydroxyproline level was determined on day 14 as described in the "Materials and methods" section. Each value represents the mean ± s.d. ($n = 5–6$). $^{**}P < 0.01$ versus control. †$P < 0.05$ versus CO-HbV.

3.2. *Effect of CO-HbV on BLM-induced pulmonary fibrosis*

To assess the effect of CO-HbV on the development of BLM-induced pulmonary fibrosis, BLM-induced pulmonary fibrosis mice were treated with saline, HbV (1000 mg Hb/kg) or CO-HbV (1000 mg Hb/kg) at 30 min prior to the BLM treatment and 1 day after BLM treatment. Mice that were administered saline or HbV showed massive weight loss in response to the BLM treatment, whereas weight loss was suppressed in the case of CO-HbV administration (Fig. 3A). Histopathological analysis (HE stain and Masson's trichrome stain) demonstrated that the BLM administration induced severe lung damage in the saline group (Fig. 3B). In addition, the BLM treatment significantly increased the hydroxyproline content of the lung as compared with the control group (Fig. 3C). These phenomena were all significantly suppressed by the CO-HbV treatment, but these effects were negligible in the case of the HbV treatment.

Moreover, to evaluate possible changes of respiratory function and lung mechanics associated with pulmonary fibrosis, we measured FVC and elastance. Based on data obtained using a computer-controlled ventilator, FVC clearly decreased in the BLM-treated mice and that this decrease was significantly suppressed by treatment with CO-HbV (Fig. 3D). The changes in lung mechanics associated with pulmonary fibrosis are characterized by an increase in elastance. Total respiratory system elastance (elastance of the total lung, including the bronchi, bronchioles, and alveoli) and tissue elastance (elastance of the alveoli) increased following BLM treatment, effects that were partially restored by the

Table 1
Plasma clinical chemistry test results in control mice and BLM-induced pulmonary fibrosis mice after saline, HbV and CO-HbV administration.

	Control	Day 7			Day 14		
		BLM + saline	BLM + HbV	BLM + CO-HbV	BLM + saline	BLM + HbV	BLM + CO-HbV
AST	34.8 ± 3.5	67.3 ± 18.5	73.7 ± 20.3	74.0 ± 24.3	61.7 ± 35.0	53.8 ± 7.3	52.9 ± 16.8
ALT	23.9 ± 3.6	46.3 ± 14.7	62.0 ± 17.3	61.0 ± 28.6	43.1 ± 21.0	33.0 ± 7.9	37.0 ± 15.1
ALP	317.9 ± 66.2	315.7 ± 106.4	302.8 ± 67.3	334.0 ± 75.8	313.8 ± 39.2	357.8 ± 54.0	324.3 ± 65.1
BUN	22.7 ± 3.7	28.3 ± 3.3	27.8 ± 5.0	30.0 ± 5.4	22.2 ± 3.3	24.1 ± 3.1	22.6 ± 1.8
CRE	0.10 ± 0.03	0.14 ± 0.02	0.10 ± 0.03	0.13 ± 0.03	0.10 ± 0.02	0.11 ± 0.01	0.10 ± 0.01
CK	105.6 ± 35.7	130.3 ± 55.6	105.2 ± 48.3	96.5 ± 29.9	224.9 ± 255.8	69.4 ± 22.1	70.3 ± 15.2
LDH	152.6 ± 42.1	301.4 ± 135.2	341.0 ± 63.6	258.7 ± 66.1	263.0 ± 141.5	278.2 ± 90.5	237.4 ± 45.0
AMY	2052.1 ± 318.2	2739.7 ± 459.7	2619.7 ± 457.1	2480.3 ± 347.4	2036.9 ± 335.1	2520.0 ± 394.6	2292.4 ± 295.7
T-CHO	125.6 ± 24.1	119.1 ± 25.9	160.7 ± 25.1	143.0 ± 23.8	127.7 ± 13.9	118.4 ± 16.4	131.3 ± 23.9

AST, aspartate aminotransferase; ALT, alanine aminotransferase; ALP, alkaline phosphatase; BUN, urea nitrogen; CRE, creatinine; CK, creatine kinase; LDH, lactate dehydrogenase; AMY, amylase; T-CHO, total cholesterol.

administration of CO-HbV (Fig. 3E and F). These results suggested that CO-HbV could be therapeutically beneficial for the treatment of BLM-induced pulmonary fibrosis.

3.3. Effect of CO-HbV on BALF cells, and inflammatory cytokines and chemokine levels in lung tissue

It is well-known that the inflammation plays an important role in the pathogenesis of IPF, in view of the presence of interstitial and alveolar inflammatory cells as well as the expression of inflammatory cytokines in the lungs of patients with IPF [33,34]. We postulated that the inhibition of pulmonary fibrosis by CO-HbV might contribute to the anti-inflammatory effect of CO [8,9]. As an indicator of inflammation, the cells in BALF were analyzed. As a result, the administration of BLM resulted in a significant increase in the number of inflammatory cells (total cells: Fig. 4A), alveolar macrophages (Fig. 4B) and neutrophils (Fig. 4C) on days 3 after BLM administration. The CO-HbV treatment significantly reduced all types of cells in the BALF.

We also examined the effect of CO-HbV on TNF-α, IL-6 and IL-1β levels in the lung tissue of BLM-induced pulmonary fibrosis at days 7. As shown in Fig. 5, the levels of TNF-α (Fig. 5A), IL-6 (Fig. 5B) and IL-1β (Fig. 5C) in lung tissue were increased by BLM were significantly decreased as the result of the CO-HbV treatment. These data suggest that CO-HbV exerts an anti-inflammatory action against BLM-induced pulmonary damage, and consequently ameliorates BLM-induced pulmonary fibrosis.

3.4. Effect of CO-HbV on ROS in lung tissue

A number of studies have suggested that the cellular redox state and the balance of oxidants/antioxidants play a significant role in the progression of pulmonary fibrosis in animal models and also possibly in human IPF [35]. To evaluate the effect of CO-HbV on ROS induced by the BLM treatment in the lung, immunostaining of 8-OH-dG and NO_2-Tyr, an oxidation product derived from nucleic acids and proteins, in lung sections were performed on day 3 after the BLM administration. As shown in Fig. 6A, the accumulation of 8-OH-dG (upper) and NO_2-Tyr (lower) in lung tissue increased in the BLM-treated mice as compared to control mice, while CO-HbV clearly suppressed the levels of these oxidative stress markers in the lungs.

Recent reports have suggested that ROS generation by the Nox family NADPH oxidases, especially Nox4, might be implicated in the pathogenesis of IPF [36,37]. In order to evaluate the ROS derived from Nox4, we examined superoxide production in lung tissue. As a result, the BLM treatment showed an obvious increase in superoxide production, Nox4 activity, while CO-HbV treatment suppressed superoxide production (Fig. 6B). However, no difference in the protein expression of Nox4 between saline and CO-HbV was found, as evidenced by immunostaining and western blotting analysis (Fig. 6C and D). Although very little is known concerning the pathway of Nox4 activity, it is well known that $p22^{phox}$ and Poldip2 are important regulators of Nox4 activity [38]. Thus, we next determined the protein expression of $p22^{phox}$ and Poldip2 at 7 days after BLM administration. Similar to the increase in the protein expression of Nox4, the protein expression of $p22^{phox}$ was also increased by BLM treatment (Fig. 6E). On the other hand, the protein expression of Poldip2 was decreased by the BLM treatment (Fig. 6F). Interestingly, no change was found in the expression of both $p22^{phox}$ and Poldip2 between the saline and CO-HbV treatment (Fig. 6E and F). These results indicate that CO derived CO-HbV suppressed the superoxide production generated by Nox4 without any detectable changes in the protein expression of Nox4, $p22^{phox}$ and Poldip2, indicating that CO suppressed Nox4 activity *via* a currently unknown pathway.

3.5. Effect of CO-HbV on active TGF-β1 levels in lung tissue

TGF-β1 has been reported to play pivotal roles in the progression of pulmonary fibrosis, including fibroblast proliferation and collagen deposition [39]. To reveal the mechanism underlying the suppressive effect of CO-HbV on BLM-induced pulmonary fibrosis, the levels of active TGF-β1 in lung tissue on day 14 were determined. As shown in Fig. 7, the level of active TGF-β1 was increased in the BLM-treated mice, while CO-HbV decreased the level of active TGF-β1 to the same level as the control group.

4. Discussion

In present study, we evaluated the therapeutic effects of CO-HbV on IPF and investigated the impact of CO on the pathogenesis of IPF using a BLM-induced pulmonary fibrosis mice model. Three major findings were uncovered in the investigation. First, CO-HbV suppressed the progression of pulmonary fibril formation and improved respiratory function. Second, the mechanism underlying the suppressive effect of CO-HbV on BLM-induced pulmonary fibrosis can be attributed to the anti-oxidative and anti-inflammatory effects of CO. Furthermore, ROS generation was decreased as the result of the inhibition of the activity of the NADPH oxidase family, which is an important role in the pathogenesis of IPF, with no detectable changes in its protein expression. Finally, it can be concluded that HbV has considerable potential for effectively delivering CO to the lungs, suggesting that CO-HbV has promise for use as an effective CO donor.

Guidance on the diagnosis and management of IPF updated by the American Thoracic Society (ATS), European Respiratory Society (ERS), Japanese Respiratory Society (JRS) and Latin American

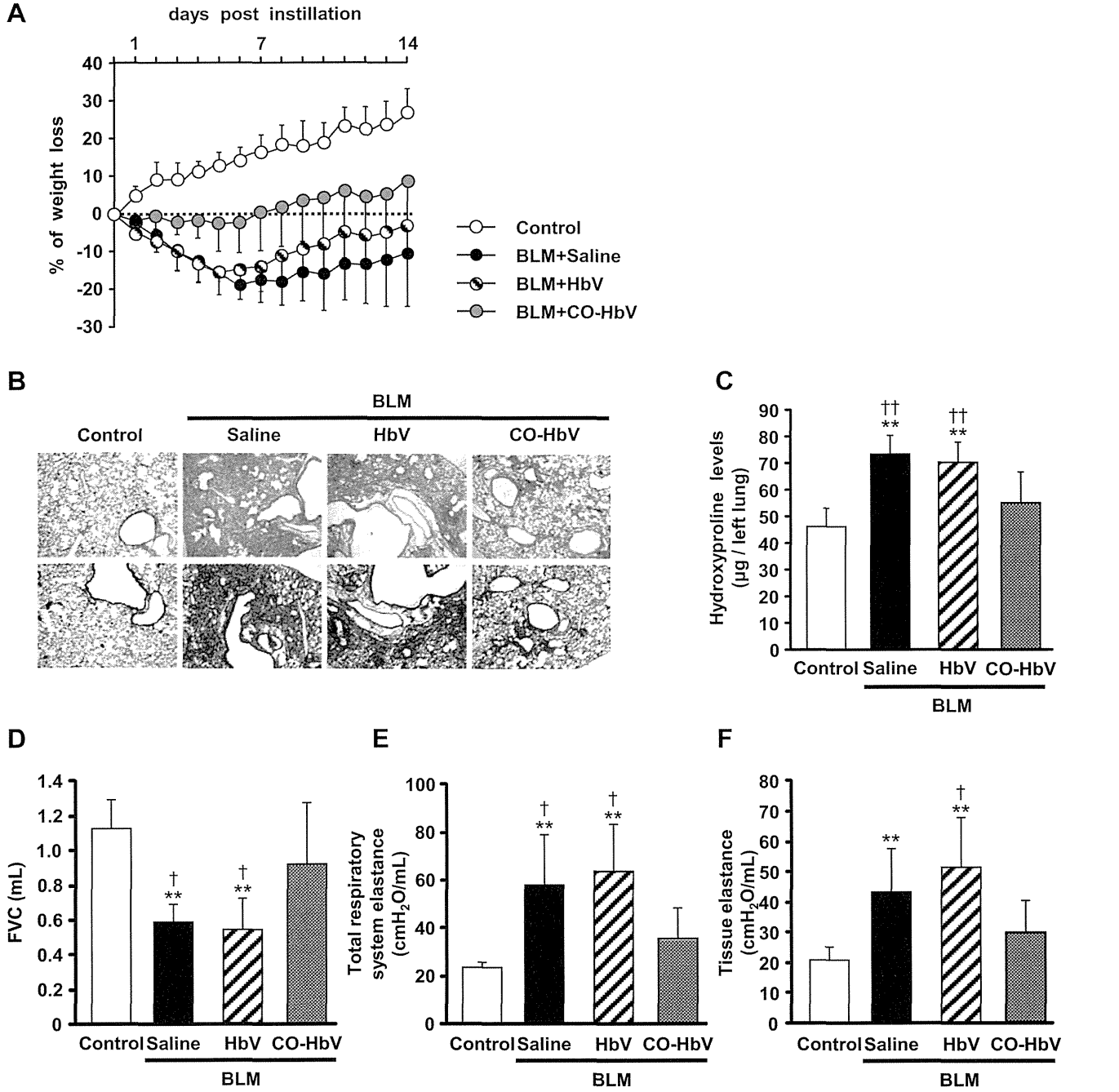

Fig. 3. Effects of CO-HbV against bleomycin-induced pulmonary fibrosis and alterations in lung mechanics. (A) The weight differences during 14 days after BLM treatment. Mice were treated with bleomycin (BLM, 5 mg/kg) once on day 0. They were also administered with saline, HbV (1000 mg Hb/kg) or CO-HbV (1000 mg Hb/kg) *via* the tail vein at 30 min before BLM treatment and 24 h after BLM treatment. Each value represents the mean ± s.d. ($n = 4–5$). (B) Histopathologic evaluation at after saline, HbV or CO-HbV treatment on day 14 in BLM-induced pulmonary fibrosis mice. Sections of pulmonary tissue were prepared on day 14 and subjected to hematoxylin and eosin staining (upper panels) and Masson trichrome staining (lower panels). (C) Hydroxyproline levels in left lung at after saline, HbV or CO-HbV treatment on day 14 in BLM-induced pulmonary fibrosis mice. The pulmonary hydroxyproline level was done on day 14 as described in Fig. 2 legend. Each value represents the mean ± s.d. ($n = 3–7$). $^{**}P < 0.01$ versus control. $\dagger\dagger P < 0.01$ versus CO-HbV. (D–F) The lung mechanics and respiratory functions at after saline, HbV or CO-HbV treatment on day 14 in BLM-induced pulmonary fibrosis mice. Forced vital capacity (D), total respiratory system elastance (E) and tissue elastance (F) were determined on day 14 as described in the "Materials and methods" section. Each value represents the mean ± s.d. ($n = 4–5$). $^{**}P < 0.01$ versus control. $\dagger\dagger P < 0.01$ versus CO-HbV. $\dagger P < 0.05$ versus CO-HbV.

Thoracic Association (ALAT) gave a 'weak no' recommendation to pirfenidon therapy, which is only drug approved for clinical use. Use of the drug can produce side effects (photosensitivity) and its effect on reducing pulmonary issues is small [40]. Therefore, it is important to examine the effect of candidate drugs on the progression of pulmonary fibrosis, lung mechanics as well as side effects. In the present study, severe pulmonary fibrosis induced by BLM was dramatically suppressed by intravenous CO-HbV administration (Fig. 3B and C). Furthermore, CO-HbV suppressed a BLM-induced increase in lung elastance and a decrease in FVC (Fig. 3D–F), indicating that CO-HbV could be beneficial for the treatment of patients with IPF. In addition, there were no changes of serum laboratory parameters reflecting hepatic, renal and pancreatic function for the experimental period after CO-HbV

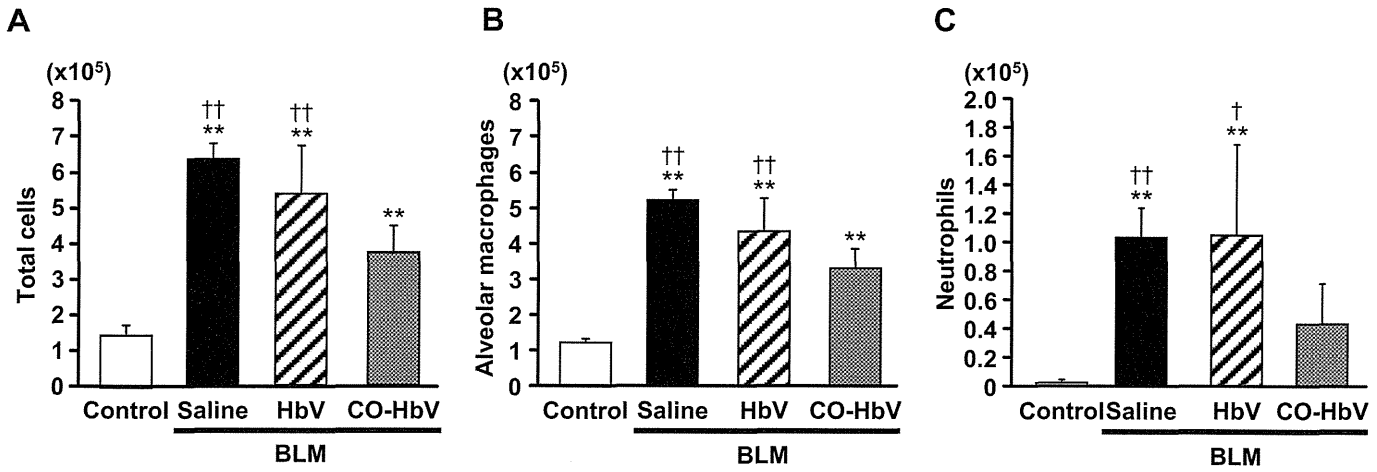

Fig. 4. Effect of CO-HbV on cells in bronchoalveolar lavage fluid in bleomycin-induced pulmonary fibrosis mice. The number of inflammatory cells including (A) total cells, (B) alveolar macrophages and (C) neutrophils in bronchoalveolar lavage fluid on day 3. These inflammatory cells were determined on day 3 as described in the "Materials and methods" section. Each value represents the mean ± s.d. ($n = 3–6$). $^{**}P < 0.01$ versus control. $\dagger\dagger P < 0.01$ versus CO-HbV. $\dagger P < 0.05$ versus CO-HbV.

administration, compared to saline treatment in BLM-induced pulmonary fibrosis mice (Table 1). However, cholesterol levels were significantly elevated at 7 days after the administration of CO-HbV. This is likely derived from metabolites contained by the HbV particles because they contain a large amount of cholesterol for structural stabilization and efficient Hb encapsulation. In a study using healthy mice and rats, we demonstrated that the added cholesterol was completely eliminated in the feces *via* biliary excretion within 14 days after the administration of HbV [41]. In fact, the serum cholesterol levels at 14 days after CO-HbV administration was not different compared to that in saline administration in this study. These results indicate that CO-HbV could suppress the progression of pulmonary fibrosis and the decline of lung mechanics without any severe side effects, thus, represents a promising candidate agent for novel IPF treatment.

Although the pathogenic mechanisms of IPF are unknown, a growing body of evidence suggests that both chronic inflammation and ROS (among other issues) appear to play a role in the onset or progression of IPF. Previous studies using human subjects with IPF have demonstrated that the generation of ROS from alveolar inflammatory cells, such as neutrophils and macrophages is enhanced and that this may promote alveolar epithelial cell injury and induce chronic inflammation, thus initiating or contributing to the development of pulmonary fibrosis [42,43]. In the present study, CO-HbV suppressed the cells count in BALF including neutrophils and alveolar macrophages (Fig. 4), and reduced the production of oxidation products (8-OH-dG and NO_2-Tyr), derived from nucleic acids and proteins, in the lung (Fig. 6A). In addition, the levels of cytokines (TNF-α, IL-6 and IL-1β) in lung tissue were significantly decreased as the result of the CO-HbV treatment (Fig. 5). It is well-known that inflammatory cells, including neutrophils and alveolar macrophages, are able to produce ROS *via* Nox2, which are essential to the development of pulmonary fibrosis in BLM-induced IPF model mice [44]. Nakahira et al. reported that ROS production was inhibited in LPS-treated macrophages when the cells were exposed to CO [45]. In addition, they also concluded that CO can form a complex with Nox2, indicating that CO is likely to modulate Nox2 activity [45]. These data suggest that CO-HbV would exert an inhibitory effect on the production of Nox2 in inflammatory cells, resulting in ameliorating the initiation and progression of BLM-induced pulmonary fibrosis.

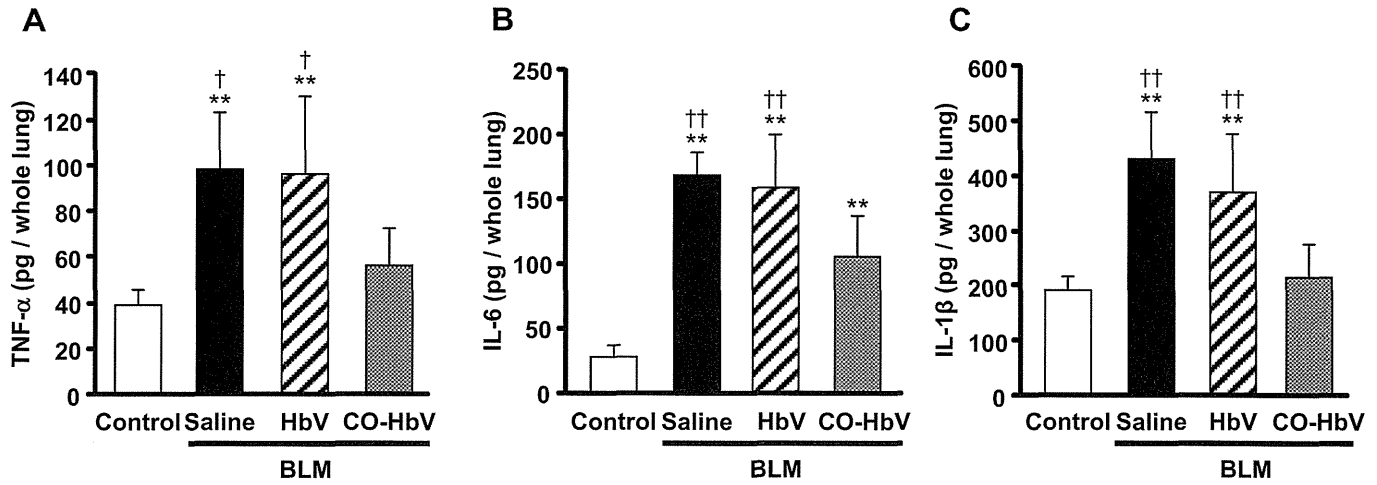

Fig. 5. Effect of CO-HbV on pulmonary inflammatory cytokines and chemokines in bleomycin-induced pulmonary fibrosis mice. The levels of cytokines and chemokine including (A) TNF-α, (B) IL-6 and (C) IL-1β in lung tissue on day 7. The amount of inflammatory cytokines and chemokine in whole lung tissue was measured by ELISA kit as described in the "Materials and methods" section. Each value represents the mean ± s.d. ($n = 5$). $^{**}P < 0.01$ versus control. $\dagger\dagger P < 0.01$ versus CO-HbV. $\dagger P < 0.05$ versus CO-HbV.

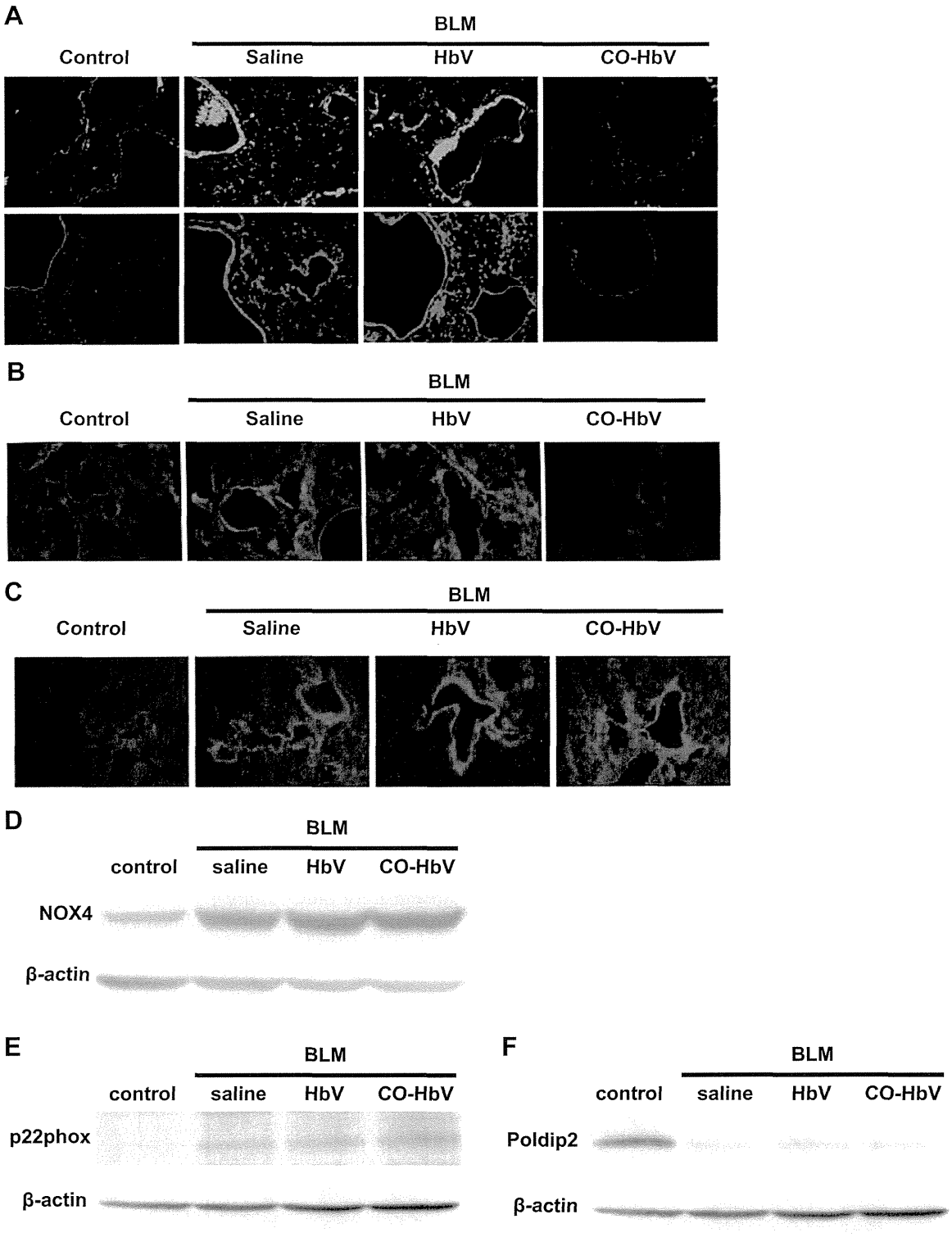

Fig. 6. Effect of CO-HbV on the generation of reactive oxygen species in lung tissue in bleomycin-induced pulmonary fibrosis mice. (A) The immunostaining of the lungs slice for the oxidative stress markers of nucleic acid (8-OH-dG; upper) and amino acid (NO_2-Tyr; lower). Mice were treated with bleomycin (BLM, 5 mg/kg) once on day 0. They were also administered saline, HbV or CO-HbV *via* the tail vein at 30 min before BLM treatment and 24 h after BLM treatment. Subsequently, the each immunostaining was performed on day 3 after BLM administration. (B) Production of pulmonary superoxide in bleomycin-induced pulmonary fibrosis mice on day 7 after BLM administration. Dihydroethidium was used to evaluate lung superoxide concentrations. (C-D)The protein expression of nicotinamide adenine dinucleotide phosphate oxidase 4 (Nox4) in lung tissue. Protein expression levels of Nox4 were determined by (C) immunostaining and (D) western blotting as described in the "Materials and methods" section. The protein expression of (E) $p22^{phox}$ and (F) polymerase delta interacting protein 2 (Poldip2)in lung tissue. Protein expression levels of both $p22^{phox}$ and Poldip2 were determined by western blotting as described in the "Materials and methods" section.

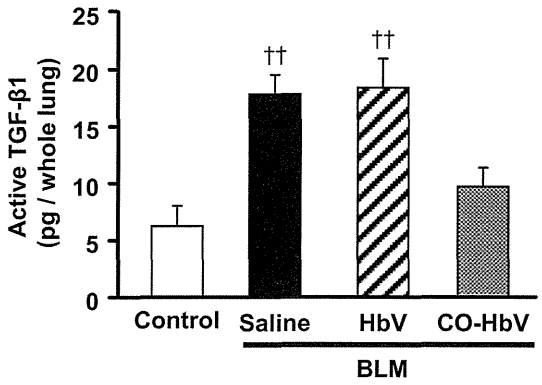

Fig. 7. Effect of CO-HbV on active TGF-β1 levels in bleomycin-induced pulmonary fibrosis mice. Active TGF-β1 levels in lung were determined on day 7 as described in the "Materials and methods" section. Each value represents the mean ± s.d. ($n = 6$). ††$P < 0.01$ versus CO-HbV.

In addition to Nox2, ROS are also generated by Nox4 and play a crucial role in the induction of alveolar epithelial cell death and the subsequent development of pulmonary fibrosis. In fact, it has been reported that Nox4 expression was increased in pulmonary fibrosis from patients with IPF [36,37], and the genetic or pharmacologic targeting of Nox4 abrogated fibrogenesis in murine models of lung injuries [37,46]. In our study, the Nox4 activity was suppressed by the administration of CO-HbV (Fig. 6B). Previously, the activity of Nox4, as determined by ROS generation, was thought to be exclusively dependent on the protein levels of Nox4 *in vitro* [47]. Interestingly, contrary with a previous *in vitro* study [47], our *in vivo* data using BLM-induced IPF model mice showed that the protein expression of Nox4 remained unchanged after the saline, HbV and CO-HbV treatment in BLM-induced IPF model mice (Fig. 6C and D). Although the activation mechanisms of Nox4 are largely unknown, at least part of the $p22^{phox}$ and Poldip2 would be related to Nox4 activity [38]. Therefore, we hypothesized that CO affected Nox4 activity *via* the membrane translocation of these two regulators, namely, $p22^{phox}$ and Poldip2. However, the protein expression of $p22^{phox}$ and Poldip2 in plasma membranes was not changed among the saline, HbV and CO-HbV treatment in BLM-induced IPF model mice (Fig. 6E and F). It therefore appears that CO inhibits a currently unknown pathway of Nox4 activation. A possible explanation for this issue is that CO interacts directly with the heme contained in Nox4. In fact, an interaction of Nox2, a heme protein, with CO was recently confirmed by a spectroscopic analysis [45]. Further investigation regarding this mechanism will be necessary to develop a comprehensive understanding of the effect of CO on tissue fibrosis.

There is an increasing body of evidence to suggest that epithelial–mesenchymal transition (EMT), a process whereby fully differentiated epithelial cells undergo a transition to a mesenchymal phenotype, thus giving rise to fibroblasts and myofibroblasts, may play a substantial role in a variety of pathogenic processes during pulmonary fibrogenesis. TGF-β1 has been implicated as functioning as a master switch in the induction of fibrosis in the lung, and is a major mediator of EMT in a number of physiological contexts, including pulmonary fibrosis [48]. In this regard, TGF-β1 is upregulated in the lungs of patients with IPF, and the expression of active TGF-β1 in the lungs of rats induces a dramatic fibrotic response, whereas an inability to respond to TGF-β1 affords protection from BLM-induced fibrosis [49]. The findings reported herein indicate that CO-HbV significantly reduced the active TGF-β1 content in lung tissue induced by the BLM treatment (Fig. 7). Several *in vitro* studies showed that ROS and inflammatory cytokines promoted TGF-β1 production in pulmonary epithelial cells and its subsequent activation [50,51]. Hence, these findings suggest that the suppression of ROS production and inflammatory cell infiltration at an early-stage of BLM treatment by CO-HbV eventually led to the suppression of active TGF-β1 production. In addition, it was reported that CO also suppressed TGF-β1-induced fibronectin and collagen production by fibroblasts and that this process was dependent, in part, on the transcriptional regulator Id1 [52]. It thus appears that CO inhibits both TGF-β1 production and some of TGF-β1 mediated signal pathways in the lung, and subsequently decreases the deposition of fibronectin and collagen, resulting in the suppression of pulmonary fibrosis.

Since the benefit of CO as a therapeutic agent has already been revealed pre-clinically in animal models of various human diseases [8], CO-HbV may not only be an effective therapeutic agent for the treatment of IPF, but also against other diseases in which the Nox family of proteins play an important role in disease progression, such as heart disease, rheumatoid arthritis, sepsis and cancer [53]. However, for clinical application of CO-HbV, there are a number of concern, particularly in relation to HbV as a carrier. Fortunately, it has already been demonstrated that HbV can be used safely as a carrier in animals, that HbV possesses a high biocompatibility, a low toxicity and does not accumulate in the body [54,55], indicating that HbV has the potential to function as a carrier of CO to diseased tissues in need of treatment without any detectable adverse effects. In addition, HbV has a good retention in the blood circulation in cynomolgus monkeys [23], and the half-life of HbV in humans was estimated to be approximately 3–4 days [56], which is long enough to function as a CO carrier. Furthermore, it is known that PEGylated liposomes show some unexpected pharmacokinetic properties, the so-called accelerated blood clearance phenomenon in which the long-circulation half-life is lost after being administered twice to the same animals [57]. Therefore, it is also concerned the pharmacokinetic properties after repeated infusion of CO-HbV, because it is expected that multiple injection of CO-HbV must be given for chronic and progressive diseases. In previous study, we demonstrated that the pharmacokinetics of HbV were negligibly affected by repeated injections at a massive dose [55].

5. Conclusions

The findings reported herein demonstrate that CO-HbV can inhibit the progression of pulmonary fibrosis. Furthermore, it can also be concluded that CO-derived anti-inflammatory and antioxidant effects are involved in its suppressive effect against pulmonary fibrosis progression and loss of lung mechanics. CO-HbV could be a new type of pharmaceutical therapeutic agent for using CO as a medical gas that would arrest ROS and inflammation-related disorders.

Acknowledgments

This work was supported in part by Health Sciences Research Grants from the Ministry of Health, Labour and Welfare of Japan (201208035) and by a Grant-in-Aid for Young Scientist (B) from the Japan Society for the Promotion of Science (JSPS) (KAKENHI 24790159).

References

[1] Bjoraker JA, Ryu JH, Edwin MK, Myers JL, Tazelaar HD, Schroeder DR, et al. Prognostic significance of histopathologic subsets in idiopathic pulmonary fibrosis. Am J Respir Crit Care Med 1998;157:199–203.
[2] King Jr TE, Tooze JA, Schwarz MI, Brown KR, Cherniack RM. Predicting survival in idiopathic pulmonary fibrosis: scoring system and survival model. Am J Respir Crit Care Med 2001;164:1171–81.